J Nanopart Res (2016) 18:291
DOI 10.1007/s11051-016-3549-0

RESEARCH PAPER

Histological and genotoxic evaluation of gold nanoparticles in ovarian cells of zebrafish (*Danio rerio*)

Navami Dayal · Mansee Thakur · Poonam Patil · Dipty Singh · Geeta Vanage · D. S. Joshi

Received: 13 June 2016 / Accepted: 1 August 2016 / Published online: 3 October 2016

Abstract Gold nanoparticles (AuNPs) have attracted a lot of attention due to their usage in consumer- and therapy-based biomedical applications. These particles are frequently the medium-sized particles within the range of 10–50 nm. A number of scientific reports have addressed the cytotoxic potential of these NPs. However, their genotoxic potential with respect to reproductive aspects remains unclear. For assessment of safety and risks associated with AuNPs to female reproductive system, adult female zebrafish *(Danio rerio)* were exposed in vivo to 20 μg/g/day of AuNPs of two different sizes. AuNPs of 15 nm (type I) and 47 nm (type II) in diameters were administered orally to female zebrafish for a period of 28 days (chronic). The ability of these AuNPs to gain access to female reproductive organs was confirmed by their accumulation pattern through inductive coupled plasma mass spectroscopy. Gonads were assessed for changes in ovarian morphology at histopathological level followed by the confirmation of bioaccumulation of AuNPs using transmission electron microscopy. Using comet assay, strand breaks in DNA of ovarian cells were investigated. Chronic exposure to type I and II AuNPs showed distinctive patterns of bioaccumulation in ovaries. Interestingly, accumulated NPs resulted in gross cellular alterations in different cell types of ovarian tissue. Comet assay analysis revealed extensive number of strand breaks in ovarian cells from the NP exposed fishes. In conclusion, AuNPs ranging between 10 and 50 nm are capable of gaining access to ovaries of zebrafish and potential enough to cause strand breaks in ovarian

N. Dayal (✉) · D. S. Joshi
Department of Medical Genetics, MGM Institute of Health Sciences, Navi Mumbai, Maharashtra, India
e-mail: navamidayal@gmail.com

M. Thakur
Department of Medical Biotechnology and Central Research Laboratory, MGM Institute of Health Sciences and College of Engineering and Technology, Navi Mumbai, Maharashtra, India
e-mail: mansibiotech79@gmail.com

P. Patil · D. S. Joshi
Department of Medical Biotechnology, MGM Institute of Health Sciences, Navi Mumbai, Maharashtra, India
e-mail: poonamparth14@yahoo.in

D. Singh · G. Vanage
National Centre for Preclinical Reproductive and Genetic Toxicology (NIRRH), National Institute of Research in Reproductive Health (ICMR), Jehangir Merwanji Street, Parel, Mumbai, Maharashtra, India
e-mail: diptyasingh@gmail.com

G. Vanage
e-mail: geetavanage@gmail.com

cells. The findings of the present study highlight the adverse effects of these NPs to female reproductive system. It opens up further avenues for research on effects of these NPs on F_1 generation descending from the exposed fishes.

Keywords Histology · Bioaccumulation · Gold nanoparticles · Zebrafish · Ovaries · Health effects

Introduction

Exposure to man-made nanosized particles is not a recent event. In the past two decades, there has been tremendous evolution in technology allowing mass production of engineered NPs. Proof-of-concept studies demonstrate various biomedical applications of AuNPs in chemical sensing (Wang and Yu 2013), biological imaging (Nune et al. 2009), and drug delivery (Ajnai et al. 2014). Concern lies in the current increase of NP usage mainly in consumer- and therapy-based applications. Drug delivery using NPs shows tremendous potential but raises concerns regarding local and systemic toxicity (Liu et al. 2009). NPs may enter the body via oral ingestion, inhalation, dermal penetration, and intravascular injection and subsequently distribute to any organ system. Once NPs enter the body, the biodistribution depends on factors like particle size (De Jong et al. 2008; Lankveld et al. 2010) and surface functionalization (Lipka et al. 2010). These particles are subject to first-pass metabolism within the liver where they may accumulate or distribute via the vasculature to end organs including the brain. Several reports suggest in vivo toxicity of AuNPs to be directly related to the size, shape, surface coating, exposure dose, and administration routes (Connor et al. 2005; Goodman et al. 2004; Zhang et al. 2009; Pan et al. 2007; Jiang et al. 2008; Pan et al. 2009; Tsoli et al. 2005; Choi et al. 2007).

The increasing demand of AuNPs has led to a strong interest in studying their potential to cause deleterious effects in biological systems, and how these effects might be mitigated. This particularly applies to reproductive aspects, where defects can be passed onto the next generations. Repotoxicological studies are a mandatory part during every stage of drug approval processes are of paramount importance as possible defects may not only affect the person or animal directly treated with the drug but also have possible adverse effects in the following generations. This is not only true for conventional drugs but also true for NPs. However, very few studies are available that have investigated the effect of NPs on female gametes (Juan et al. 2009; Hsieh et al. 2009; Tiedemann et al. 2014). The genetic integrity of the gonads is an essential aspect for reproductive success. It is, therefore, necessary to detect DNA alterations in cells of the reproductive tissue.

Despite of its noticeable importance, testing of NPs for reproductive toxicity has been neglected. Cytotoxic and genotoxic potential of NPs have been demonstrated in most of the in vitro studies. To clarify these effects, the implementation of in vivo studies has been undertaken using zebrafish as a model for reproductive toxicity assessments of AuNPs. In the present study, we investigate the effects of AuNPs of two different sizes, i.e., 15 and 47 nm on female reproductive system of zebrafish after repeated dosing for 28 days (chronic study). For this purpose, concentration of gold accumulated in ovaries of zebrafish was estimated using inductive coupled plasma mass spectroscopy (ICP-MS). The study demonstrates alterations in ovarian morphology at histological level followed by confirmation of bioaccumulation at ultrastructural level using transmission electron microscopy (TEM). In addition, it also highlights the extent of strand breaks induced by these NPs in ovarian cells based on alkaline comet assay.

Materials and methods

The present study is a type of randomized controlled trials investigating the effects of AuNP on reproductive system of zebrafish.

Synthesis and characterization of AuNPs

AuNPs within the size range of 10–20 nm (type I) were produced following the procedure of Turkevich et al. (1951) and Rathore et al. (2014) while AuNPs within the size range of 40–50 nm (type II) were produced with few modifications in the procedure of Abdelhalim and El-Toni (2012). This chemical reduction method for NP synthesis used

tetrachloroaurate as metal salt and trisodium citrate as reducing agent. Trisodium citrate, used as reducing agent, also has the property to stabilize the AuNPs in solution. Thus, no additional stabilizer or other component was used in this research to prevent agglomeration of AuNPs. The size and shape of the NPs were confirmed using transmission electron microscopy (Philip, Model No.CM200, Operating voltages: 20–200 kv resolution 24 A°). The solution was found to be stable for over 2 months when stored at 4 °C.

Adult fish conditions

The experimental set-up consisted of 12 rectangular tanks (5 L volume) maintained at the Zebrafish facility of MGM Central Research Laboratory. Initial system and replacement water was obtained by filtering tap water through a 1-μm string filter and activated charcoal filter followed by reverse osmosis (RO) using Kent Maxx (Model no. KR131012830). Tank water was constantly aerated. Water pH ranged between 8.0 and 8.3., and ammonia–nitrogen and NO_2–N remained below level that can be detected visually by test color variation. Water temperature was maintained at 28 ± 1 °C and monitored daily using a thermometer. In addition, water quality (pH, turbidity, chloride, total hardness, fluoride, nitrate, iron and residual chlorine) was monitored weekly using a multiparameter water testing kit.

All animal experiments were conducted with prior approval from MGM's Medical College, Institutional Animal Ethics Committee. Indigenous wild-type zebrafish strains were maintained at the Zebrafish facility of MGM Central Research Laboratory. All procedures for maintenance and care of zebrafish were as per The Zebrafish Book (Westerfield 1994). Adult zebrafish (females weighing 0.4–0.6 gm body weight) were used in the age group of 4–5 months. Fishes were fed twice a day by local fish feed and once with live artemia cysts as a source of proteinaceous feed. They were maintained on a 14:10 h light:dark cycle in a room.

A total of 120 female fishes were randomly divided into twelve groups comprising of four control groups and eight test groups for each assay. Each group included ten fishes. The detailed description of experimental groups is as follows:

Group 1-bioaccumulation studies

Group 1A-control group ($n = 10$)
Group 1B-15 nm AuNP test group ($n = 10$)
Group 1C-47 nm AuNP test group ($n = 10$).

Group 2-histopathology studies

Group 2A-control group ($n = 10$)
Group 2B-15 nm AuNP test group ($n = 10$)
Group 2C-47 nm AuNP test group ($n = 10$).

Group 3-transmission electron microscopy studies

Group 3A-control group ($n = 10$)
Group 3B-15 nm AuNP test group ($n = 10$)
Group 3C-47 nm AuNP test group ($n = 10$).

Group 4-genotoxicity assessments

Group 4A-control group ($n = 10$)
Group 4B-15 nm AuNP test group ($n = 10$)
Group 4C-47 nm AuNP test group ($n = 10$).

Fishes from the test groups received approximately 100 μl of AuNP solution at the dose of 20 μg/g/day for 28 days via oral administration (Dayal et al. 2016a, b). This dose was determined based on the LC_{50} value obtained through preliminary screening experiments performed on zebrafish embryos. Briefly, in this assay, a generation of zebrafish embryos ($n = 10$ embryos for each NP test concentration) were exposed to different concentrations of AuNPs at approximate 4 hpf and monitored till 96 hpf. LC_{50} value was calculated based on percent mortality at 96 hpf which was obtained at 20 μg/ml for both type I and II AuNPs. In contrast, the control groups were administered with equal volume of distilled water as AuNPs were prepared and suspended in distilled water. On day 29, fishes were sacrificed by anesthetizing them in ice water and dissected to obtain ovaries.

Gold quantification in ovaries

Measurement of gold in gonads was carried out after 28 days of exposure (Note: The organs from three fish in each test were clubbed to obtain enough tissue for estimation purpose). At the end of exposure, the fishes were sacrificed. Immediately after dissection and prior

to digestion, tissues were rinsed in three successive baths containing distilled water, placed in an aluminum pan, and dried until constant mass in a dry heat oven (at least 48 h at 55 °C). After cooling, they were weighed using a weighing balance (Contech Company, CA:123-1101815). Tissues were then digested following the acid digestion protocol (Moor et al. 2001). The digested samples were analyzed for presence of gold in respective organs using ICP-MS technique (Make: Element XR, Model: Thermo Fisher Scientific, Germany). The value estimated through ICP-MS in each digested sample was used to determine gold content in µg/g organ weight. All statistical analysis was performed using Statcalc3 version 4.0 software. One-way ANOVA was applied to calculate significance of difference between the control and treated groups and between two test groups.

Histopathological studies

Histological examination was performed following 28 days of chronic exposure. For this purpose, the fishes were anesthetized in ice water and dissected to obtain ovaries. The organs were fixed in 10 % formalin for 24 h at room temperature. Fixed tissue was dehydrated and embedded in the paraffin wax. Serial cross sections of 5 µm were cut by microtome (Leica RM255) and stained with hematoxylin and eosin (H & E). The samples were examined under the light microscope (Olympus Magnus, Model no. 11F589). Staging of germ cells was observed as described by Menke et al. (2011).

Ultrastructural studies

For this purpose, the fishes from the control and the test groups were collected for ultrastructural analysis. In order to obtain the ovaries, the fishes were anesthetized and dissected. Ovaries were dissected and fixed in modified Karnovsky's fixative (4 % glutaraldehyde, 4 % paraformaldehyde, 0.2 % picric acid, 0.02 % calcium chloride, 0.2 M cacodylate buffer). Further, the tissues were postfixed in 1 % osmium tetroxide in the same buffer, dehydrated in graded acetone solutions, and embedded in resin (araldite). Rinsing, postfixation, dehydration, and infiltration were carried out in the KOS microwave tissue processor (Milestone). The ultrathin sections for the TEM analysis (60 nm) were obtained using a Leica Ultracut R ultramicrotome (Leica Microsystems, Milton Keynes, England). The ultrathin sections were then stained with 2 % alcoholic uranyl acetate and Lead citrate for 10 min in the dark, thoroughly washed in Milli Q water, and allowed to air dry before examination. For ultrastructural analysis, the copper grids containing the stained ultrathin sections were observed under Transmission Electron Microscope (TECNAI, FEI) using an accelerating voltage of 120 kV equipped with a CCD camera.

Comet assay

In each test group and the control, organs of 3 fishes were pooled. For cell isolation, protocols by Braunbeck and Storch (1992) and Schnurstein and Braunbeck (2001) for preparation of primary hepatocytes and gill cells in comet assay was applied. Briefly, ovaries from female zebrafish were dissected and rinsed in 1X PBS, pH 7.2. The tissue was separately incubated in 1X PBS, pH 7.2 and gently teased to release single cells. Filtration step was omitted for female gonads in order to avoid destroying larger oocytes. Cells were then centrifuged for 10 min at 100 g and 20 °C. The cell pellet was then resuspended in chilled 1X PBS, pH 7.2 supplemented with 10 % fetal calf serum at a density of 10^5 cells/ml.

Cells were checked for viability before the start of the experiment using the Trypan blue dye exclusion test (Strober 2001). Comet assay detecting the DNA strand breaks (single- and double-strand breaks, and alkali labile sites) was performed under alkaline conditions according to Singh et al. (1988) with modifications detailed by Schnurstein and Braunbeck (2001). Lysis conditions followed the protocol by Kosmehl et al. (2004). The cells were centrifuged at 1200 rpm/10 min, and cell pellet was resuspended in chilled 1X PBS, pH 7.2. The suspension (20 µl) was then mixed with 130 µl normal melting agarose (NMA) and placed on a fully frosted microscopic slide precoated with a layer of 1 % low melting agarose (LMA). The microscopic slide was then immersed in cold (4 °C) lysis solution. (2.5 M NaCl, 100 mM EDTA, 10 mM Trizma Base. Adjust pH to 10) containing freshly added 1 % Triton X-100 and 10 % DMSO. After an hour, the slides were dipped in freshly prepared alkaline buffer (1 mM Na_2EDTA and 300 mM NaOH, pH 13) for 20 min to allow DNA

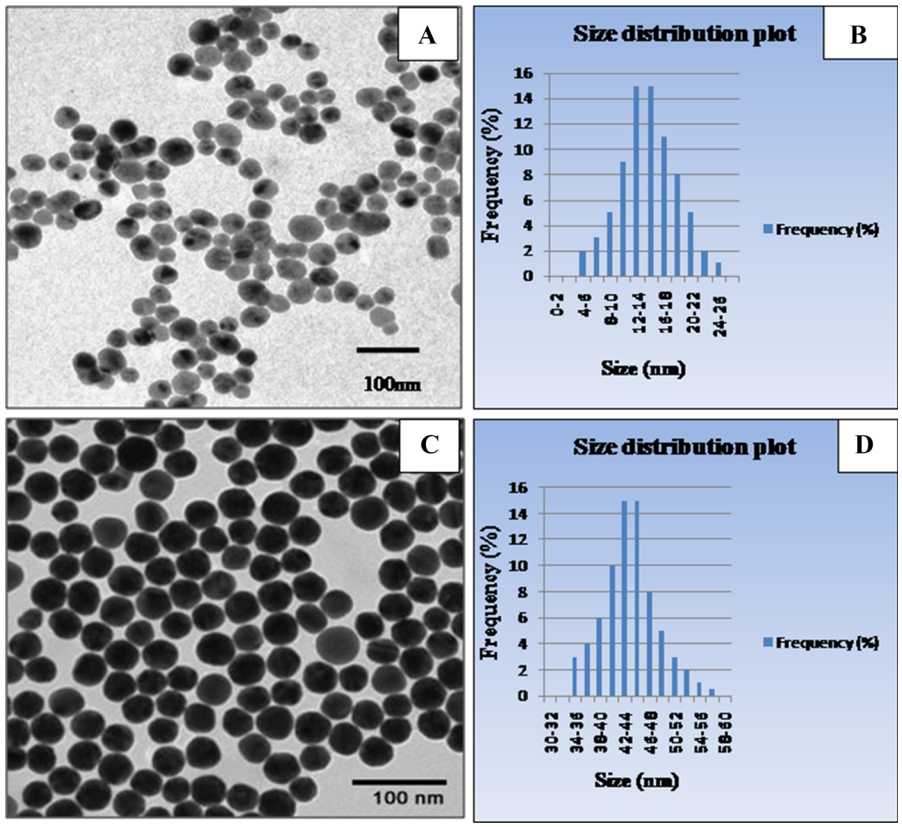

Fig. 1 TEM micrographs and size distribution plots for AuNPs formed through chemical reduction method. **a** and **b** TEM image and size distribution plot for AuNPs indicating the average size diameter to be 15 ± 6.6 nm. **c** and **d** TEM image and size distribution plot for AuNPs indicating the average size diameter to be 47 ± 7.7 nm

unwinding. Electrophoresis was performed at 50 V for 15–30 min. The slides were finally neutralized with a 0.4 M Tris Buffer, pH 7.5 and stained with 100 µl ethidium bromide (10 µg/ml). Observations were made at a magnification of ×400 using an inversion fluorescence microscope (Zeiss) equipped with a 530 nm excitation filter, a 590 nm emission filter, a digital camera, and a comet imager 2.2 analysis software. More than 50 cells from each slide were randomly selected for data analysis of DNA damage percentage in the tail. Experimental data are represented in the form of box and whisker plot.

Statistical analysis

All statistical analysis on experimental data from comet assay was performed using Statcalc3 version 4.0. One-way ANOVA was used to analyze the significant difference between groups at $p < 0.05$.

Results

Synthesis and characterization of AuNPs

The type I and II AuNPs in the colloidal solution are negatively charged due to the presence of citrate ions coated over its surface. Therefore, they repel each other and stay upended in solution. On characterization using transmission electron microscopy, the mean diameter of type I and II AuNPs were 15 ± 6.6 and 47 ± 7.7 nm, respectively. The TEM micrographs and size distribution plots for NPs are shown in Fig. 1.

Gold content estimation in ovaries

The results of gold bioaccumulation in ovaries of females after chronic exposure to AuNPs of average sizes 15 and 47 nm are presented in Fig. 2. Statistical analysis showed a significant accumulation of AuNPs

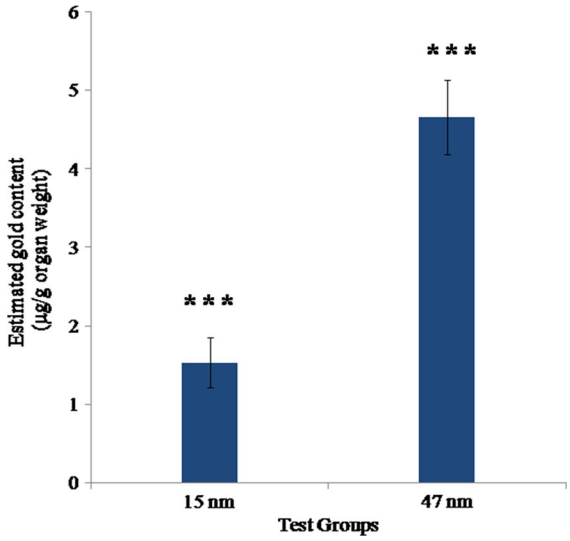

Fig. 2 AuNP accumulation in fish ovaries at the end of chronic exposures to by ICP-MS. Gold content estimated in control groups were below detectable limits. Data are represented as mean ± SE. One-way ANOVA was applied using Statcalc 3 version 4.0 software to determine statistically significant differences between control and test groups (***$p < 0.001$)

at the end of chronic exposure. Gold content estimated in ovaries was found to be 1.53 and 4.66 µg/g organ weight for 15- and 47-nm AuNP exposed groups respectively. However, a significant NP size-dependent response was observed with increase in the uptake of 47-nm AuNPs compared to AuNPs of 15 nm.

Histopathological examination of ovaries

Six blocks per group were prepared and 10–12 sections per block per observed. Histopathological studies showed normal development of gametogenic populations in the control group. In ovaries of female zebrafish under control group (Fig. 3a–c), oocyte/vitellin membrane in the vitellogenic stage appeared regular and intact with easily distinguishable zona radiata and follicular epithelium to the exterior. At every stage of development, there is a proportional increase in the size of the follicles. In the perinucleolar stage (PS), multiple nucleoli were observed at the periphery in the nucleus of the oocytes. The follicle layers were not entirely developed, but they were visible. The follicles at this stage of development were comparatively smaller in diameter. In the cortical alveolus stage (CaS), the ooplasm gets filled with granular structures called cortical alveoli. At this stage, the zona radiate begins to form and the follicular epithelial cells appear to form to the exterior. The next stage of development is the vitellogenic stage (VS), and vitellogenesis is seen in the developing follicles. At the final stage of oocyte development, i.e., mature stage (MS), marked vitellogenesis is observed in the matured oocyte. Outside the membrane, the follicular epithelial cells were seen with their uniformly arranged nuclei.

For female fishes exposed to AuNPs of 15 nm, histology of ovaries showed detachment of zona radiata from oocyte membrane in oocytes at vitellogenic and mature stage (marked with red arrow heads). However, this condition was not seen in primary and cortical alveoli stage (Fig. 2b). Few atretic oocytes (AO) were also observed particularly in the mature oocyte stage (Fig. 3e, f). Similarly, for female fishes exposed to AuNPs of 47 nm, oocytes in primary and cortical alveolar stage appeared normal (Fig. 3g). Atretic oocytes could be seen in both vitellogenic and mature staged oocyte (Fig. 3h, i). Irregularity in cell layers could be seen for both the test groups. The number of atretic oocytes quantified for controls were less than 5 %. In case of experimental groups, ovaries of 15-nm AuNP-treated fishes showed 25.01 % and those of 47-nm AuNP-treated fishes showed 25.22 % atretic oocytes.

Ultrastructural examination of ovaries

Figure 4a–d shows the representation of electron micrographs of control group. Figure 4a shows an oocyte in its vitellogenic stage (VS) with an intact membrane showing distinct cell layers of theca cells (Th), granulosa cells (Gr), and the zona radiata (ZR). Figure 4b–d shows oocyte in their primary oocyte (PS), cortical alveoli (CaS), and mature oocyte stage (MS), respectively. Multiple nucleoli (No) could be observed in primary oocyte stage as shown in Fig. 4b. Oocyte in Fig. 4c indicates cortical alveoli stage with appearance of granular ooplasm. Mature oocytes showed presence of yolk proteins (Y) and lipid droplets (L) as indicated in Fig. 4d. There were no obvious degenerative changes observed at ultrastructural level in all the above-mentioned stages of oocytes examined. In contrast, remarkable bioaccumulation of AuNPs (marked by arrow heads) was seen in the ooplasm of both test groups as observed in Fig. 4e and f. Electron micrographs of ovary of 15-nm AuNP-

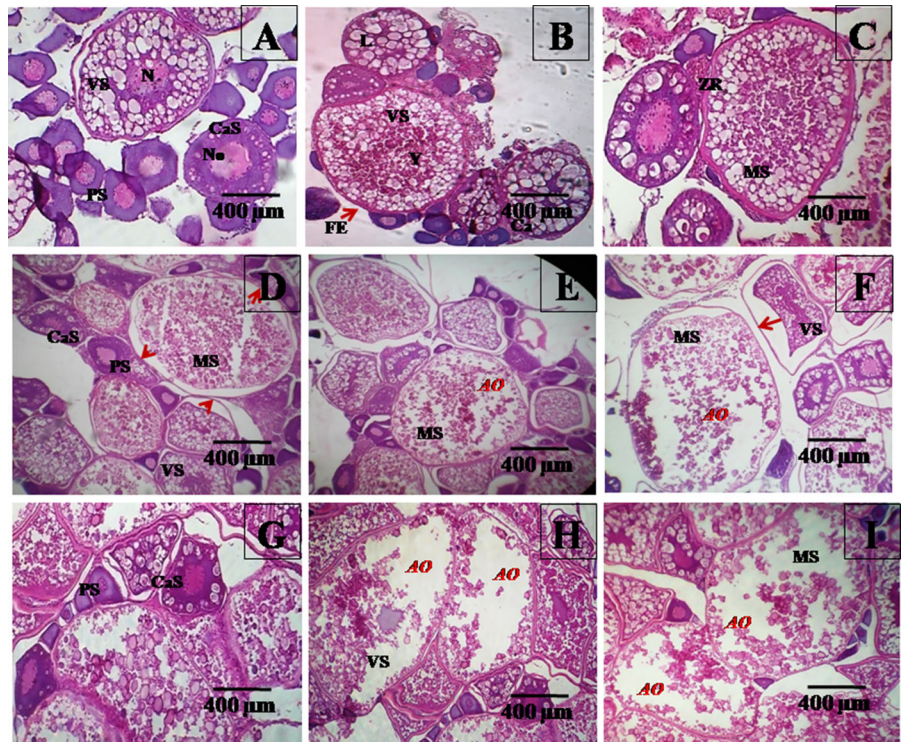

Fig. 3 Histological sections of zebrafish ovaries under 100X magnification of optical microscope **a**, **b**, and **c** Oocytes in different stages of development in control group. O-Ooplasm, No-Nucleolus, N-Nucleus, PS-Primary stage, CaS-Cortical alveoli stage, Y-Yolk, VS-Vitellogenic stage, ZR-Zona radiata, FE-Follicular epithelial cells and MS-Mature stage. **d**, **e**, and **f** Oocytes in different stages of development in 15-nm AuNP test group. Primary and Cortical alveoli stage of the oocyte appear normal. Atretic oocytes (AO) can be observed in oocytes at mature stage. Membrane detachments were also seen as marked by red arrow heads. **g**, **h**, and **i** Oocytes in different stages of development in 47-nm AuNP test group. Primary and Cortical alveoli stage of the oocyte appear normal. Vitellogenic and Mature oocytes showed gross degenerative changes

treated female fishes showed abundant AuNPs aggregates within and surrounding the cortical alveoli as seen in Fig. 4f at higher magnification than Fig. 4e. Degenerated granulosa cells and accumulation of 47-nm AuNPs in the follicular epithelium of zona radiata can be observed in Fig. 4g. This marks the ability of 47 nm AuNPs also, to damage the granulosa cells of the oocyte membrane and enter the oocytes. Figure 4h indicates accumulated NPs around the surface of the lipid vesicles. Apart from bioaccumulation of NPs, degenerative changes were noted at ultrastructural level in both the test groups (marked by (*) denotation).

Genotoxicity assessment in ovarian cells

Accumulation of AuNPs in female ovaries led to investigate their toxicity to female reproductive system. Genotoxicity assessments were carried out to understand the effects of these accumulated NPs on ovarian cells. The extent of strand breaks in ovarian cells was evaluated using comet assay based on calculating the percentage of tail DNA. For ovaries analyzed from the control group, the proportion of DNA in the tail of ovarian cells from control group was 12 %. The appearance of nucleoids from control group is shown in Fig. 5a–c. Ovarian cells from fish exposed to 15- and 47-m AuNPs, respectively, showed significant extent of strand breaks. The average extent of strand breaks found in ovarian cells was 51 % (Fig. 5d–f) and 53 % (Fig. 5g–i) for AuNPs of average sizes 15 and 47 nm, respectively. Statistical analysis using ANOVA showed significant difference in percentage of tail DNA for ovarian cells from both the test groups as compared with that of control group. However, the DNA damage levels did not differ significantly between the two test groups. Percentage of tail DNA is represented in the form of box and whisker plot as described in Fig. 6.

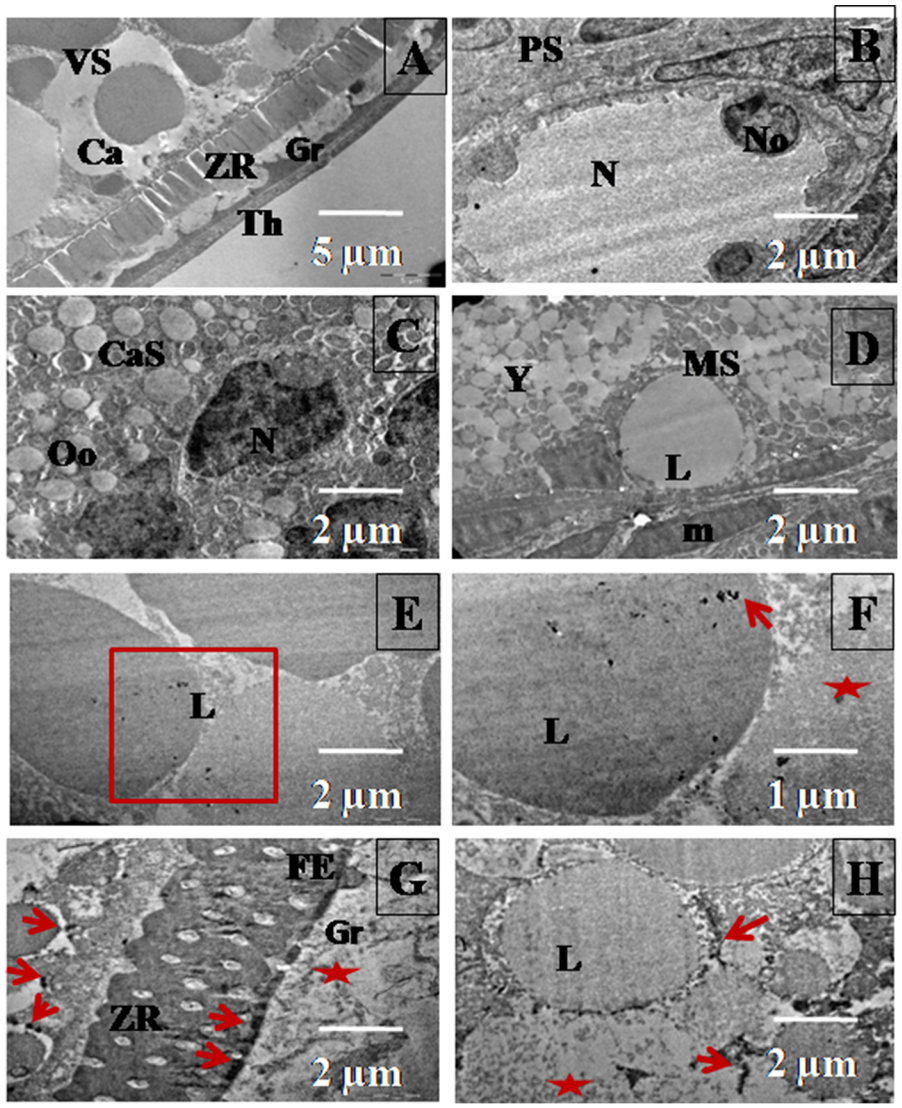

Fig. 4 Histological sections of zebrafish ovaries from control (**a**, **b**, **c**, and **d**) and test (**e**, **f**, **g**, and **h**) groups under transmission electron microscope. **a** Vitellogenic stage oocyte with an intact membrane showing distinct cell layers of theca cells (Th), granulosa cells (Gr), and the zona radiata (ZR); *Scale bar* = 2 µm. **b** Oocyte in its primary growth stage (PS) showing multiple nucleoli; *Scale bar* = 2 µm. **c** Vitellogenic stage oocyte (VS); *Scale bar* = 2 µm. **d** Mature stage oocyte with yolk (Y) and lipid (L) molecules in the ooplasm; *Scale bar* = 2 µm. **e** Ovary of zebrafish from 15-nm AuNP test group. Oocyte in the vitellogenic stage showing accumulated NPs within and surrounding the lipid vesicles (L); *Scale bar* = 2 µm. **f** Higher magnification of image (**e**); *Scale bar* = 1 µm. **g** and **h** Ovary of zebrafish from 47 nm AuNP test group. Degenerated granulosa cells (Gr) are shown in image (**g**). Mature oocytes showing NPs surrounding the surface of the lipid vesicles (**L**) and the follicular epithelium of zona radiata are indicated in image (**h**); *Scale bar* = 2 µm

Discussion

Toxicity potential of metal NPs have been investigated in rats and found to induce toxicity (Rathore et al. 2014). However, there still remain inconsistencies in the reported findings several recent review articles examining the current literature suggest a number of factors that could contribute to the inconsistent results (Doak et al. 2009; Singh et al. 2009). The studies presented here demonstrate a rapid, reliable, and cost-effective model for reprotoxicity studies. Through this study, we have gained insights into the importance of

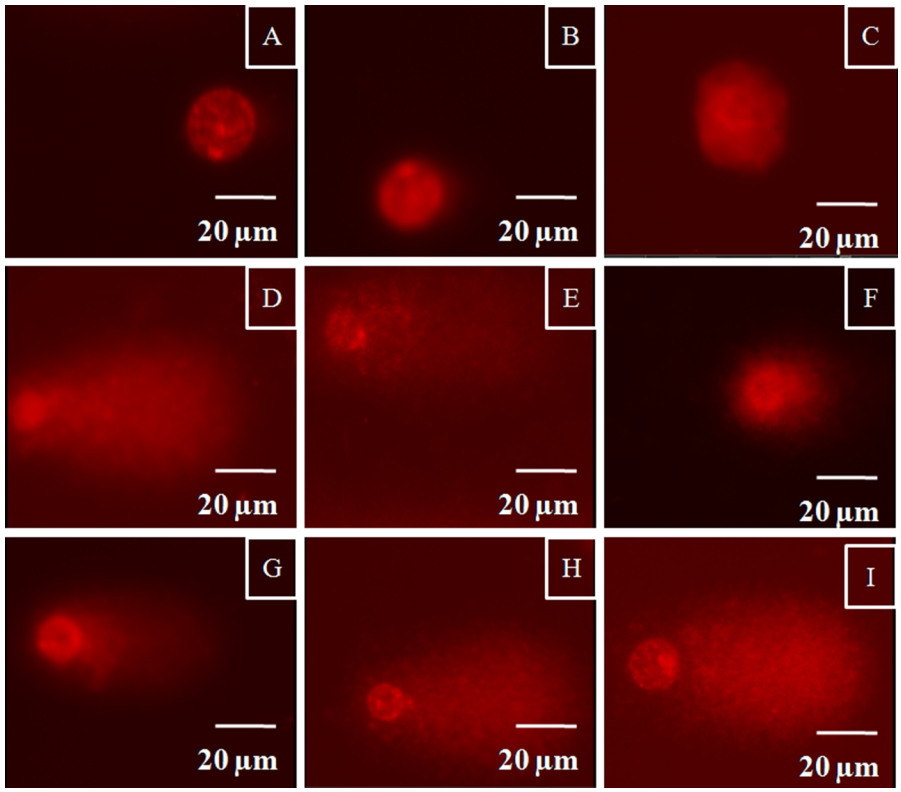

Fig. 5 Nucleoids of ovarian cells from zebrafish indicating significant levels of DNA damage after 28 days of exposure to type I & II AuNPs in vivo based on fluorescence microscopy **a**, **b**, and **c** control group indicating a normal nucleoid having a round head without a tail; **d**, **e**, and **f** ovarian cells of zebrafish exposed to 15-nm AuNPs indicating nucleoids that contain a large tail like a comet and a small head; and **g**, **h**, and **i** ovarian cells of zebrafish exposed to 47-nm AuNPs indicating nucleoids with a large tail and a small head

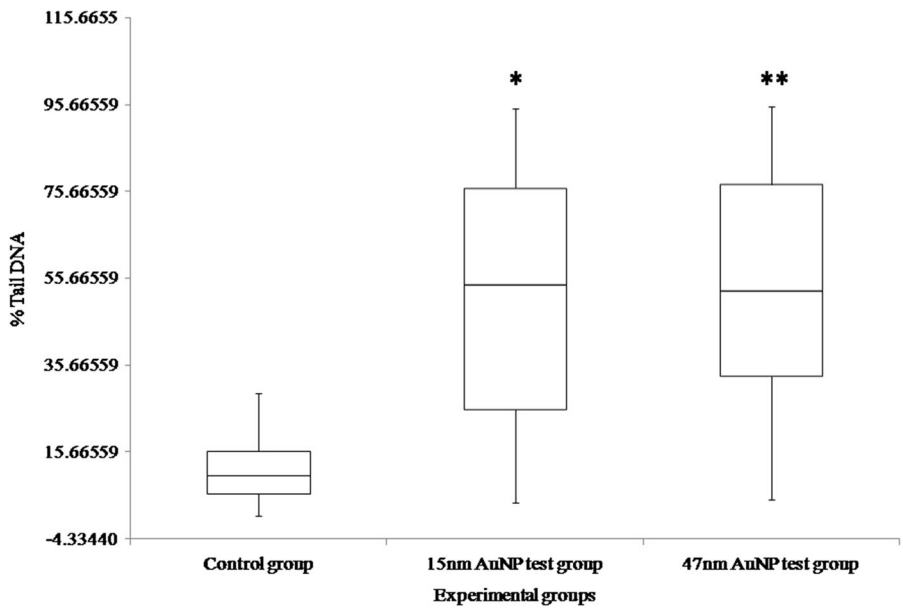

Fig. 6 Percentage of comet tail DNA in ovarian cells of zebrafish after 28 days of exposure to type I & II AuNPs in vivo. Data are given as median within box plots displaying the following percentiles: 25 and 75 (box) as well as 10 and 90 (whiskers). $*p < 0.05$ and $**p < 0.01$ represent statistically significant differences from control

AuNPs that govern their interactions with female biological system. To our knowledge, this is the first report to show female reproductive toxicity in vivo associated with AuNPs of varying sizes using zebrafish as a model. The idea of using zebrafish for reproductive toxicity assessments has recently been adopted by scientists (Ramsden et al. 2013; Wang et al. 2011; Bourrachot et al. 2014). The current study suggested that AuNPs of average sizes 15 and 47 nm showed accumulation in female gonads. Such accumulation resulted in gross alterations in ovarian cells as evident from histopathological analysis (Fig. 3) and ultrastructural analysis (Fig. 4). There are very few studies available that have reported the effects of NPs on female gametes. Recently, Tiedemann et al. (2014) investigated the response of oocyte complexes to BSA-coated AuNPs. However, these studies were carried out in vitro. The particles were found to be internalized in large numbers into the oocytes but did not show any manifestation on oocyte maturation (Tiedemann et al. 2014). Juan et al. (2009) examined the effect of TiO_2 NPs on isolated prenatal rat follicles in vitro, while Hsieh et al. (2009) studied the cytotoxicity of CdSe quantum dots on the maturation of mouse oocytes, fertilization, and fetal development. Both these studies reported detrimental effects of NPs on oocyte maturation. These reports suggest that female gametes are presently at risk when exposed to nanoscale materials.

Bioaccumulation of AuNPs in reproductive organs may induce DNA damage. For this purpose, genotoxicity assessments were carried out using comet assay. The findings in the present study reported presence of strand breaks in ovarian cells (germ cells as well as other cell types). This could be one of the causes for degenerative changes and altered reproductive performance in exposed females. In recent years, studies have evaluated the potential adverse effects of NP exposure on DNA damage to cells of female reproductive system. Zhu et al. (2009) demonstrated toxic effects of TiO_2 NPs on CHO cells resulting in DNA strand breaks. Ha Ryong Kim et al. (2013) observed DNA breakage and micronucleus formation in CHO cells stimulated by AgNPs. With regard to overall toxicity, our results agree with the general conception of impairment of the female reproductive function due to metal-based NPs and QDs (Gao et al. 2012; Ramsden et al. 2013; Stelzer and Hutz 2009). Wang et al. (2011) reported chronic exposure to 0.1 mg/L of TiO_2–NPs can significantly impair zebrafish reproduction in females. Interestingly, exposure to identical concentrations of NPs but for a shorter duration showed a normal spread of oocyte development in female gonads from all exposed groups of zebrafish (*Danio rerio*) (Ramsden et al. 2013). Similar observations were noted by our group in a study carried out for a subacute exposure period in zebrafish (Dayal et al. 2016a, b). In a study carried out by Griffitt et al. (2012) to investigate the effect of AgNPs in minnows, gene expression analysis revealed dramatic transcriptional response indicating that exposure to AgNPs has the potential to cause reproductive dysfunction even in the absence of ovary morphological and developmental alterations. These studies demonstrate NPs can interfere with normal female reproductive function by inducing cytotoxic effects on ovarian structural cells, impairing oogenesis and follicle maturation, and altering normal sex hormone levels.

Conclusions

In conclusion, our results reveal that irrespective of size of AuNPs (whether 15 or 47 nm), there are obvious adverse effects to reproductive organs of female zebrafish under chronic exposure conditions. The present study shows genotoxicity and gross degenerative changes observed in ovarian morphology at histopathological and ultrastructural level that were significantly influenced due to accumulation of AuNPs in ovaries. The findings in the present study open up further avenues for research on effects of these NPs on F_1 generation descending from the exposed fishes.

Acknowledgments The authors would like to thank MGM Institute of Health Sciences for providing the infrastructure. The authors thank Mr. Runit Patil, Laboratory Attendant for his efforts in maintenance of the zebrafish facility.

Authors' contributions Ms. Navami Dayal is a PhD student who conducted the experimental part comprising of synthesis and characterization of AuNPs, histopathology, and comet assay under the supervision of Dr. Mansee Thakur. Ms. Dayal also contribute to manuscript preparation. Dr. Dipry Singh conducted the electron microscopy analysis of zebrafish ovaries. Ms. Poonam Patil carried out all the dissection process of zebrafish and assisted Ms. Dayal in comet assay procedure. Comet assay procedure was conducted under the guidance and expertise of Dr. Geeta Vanage. Dr. D. S. Joshi contributes to conception of the research work and shares his expertise in nanotechnology.

Compliance with ethical standards

Conflict of Interest The authors declare no conflict of interest.

References

Abdelhalim MAK, El-Toni AM (2012) Optimization of a citrate method for synthesizing GNPs of controllable particle size and monodispersity: physical studies. Open Access Scientific Reports 1(5):1–5

Ajnai G, Chiu A, Kan T, Cheng CC, Tsai TH, Chang J (2014) Trends of gold nanoparticle-based drug delivery system in cancer therapy. J Exp Clin Med 6(6):172–178

Bourrachot S, Brion F, Pereira S, Floriani M, Camilleri V, Cavalié I, Adam-Guillermin C (2014) Effects of depleted uranium on the reproductive success and F1 generation survival of zebrafish (*Danio rerio*). Aquat Toxicol 154:1–11

Braunbeck T, Storch V (1992) Senescence of hepatocytes isolated from rainbow trout (*Oncorhynchus mykiss*) in primary culture. Protoplasma 170(3–4):138–159

Choi HS, Liu W, Misra P, Tanaka E, Zimmer JP, Ipe BI, Frangioni JV (2007) Renal clearance of quantum dots. Nat Biotechnol 25(10):1165–1170

Connor EE, Mwamuka J, Gole A, Murphy CJ, Wyatt MD (2005) Gold nanoparticles are taken up by human cells but do not cause acute cytotoxicity. Small 1(3):325–327

Dayal N, Thakur M, Soparkar A, Doctor M, Patil P, Joshi DS (2016a) Effective method to deliver test substance in adult zebrafish. Int J Adv Res 4(7):543–551

Dayal N, Thakur M, Patil P, Swain N, Joshi DS (2016b) Effects of subacute exposure to gold nanoparticles on germ cells of zebrafish (*Danio rerio*): an in vivo study. MGM J Med Sci 3(1):1–6

De Jong WH, Hagens WI, Krystek P, Burger MC, Sips AJ, Geertsma RE (2008) Particle size-dependent organ distribution of gold nanoparticles after intravenous administration. Biomaterials 29(12):1912–1919

Doak SH, Griffiths SM, Manshian B, Singh N, Williams PM, Brown AP, Jenkins GJS (2009) Confounding experimental considerations in nanogenotoxicology. Mutagenesis 24:284–293

Gao G, Ze Y, Li B, Zhao X, Zhang T, Sheng L, Cheng J (2012) Ovarian dysfunction and gene-expressed characteristics of female mice caused by long-term exposure to titanium dioxide nanoparticles. J Hazard Mater 243:19–27

Goodman CM, McCusker CD, Yilmaz T, Rotello VM (2004) Toxicity of gold nanoparticles functionalized with cationic and anionic side chains. Bioconj chem 15(4):897–900

Griffitt RJ, Brown-Peterson NJ, Savin DA, Manning CS, Boube I, Ryan RA, Brouwer M (2012) Effects of chronic nanoparticulate silver exposure to adult and juvenile sheepshead minnows (*Cyprinodon variegatus*). Environ Toxicol Chem 31(1):160–167

Hsieh MS, Shiao NH, Chan WH (2009) Cytotoxic effects of CdSe quantum dots on maturation of mouse oocytes, fertilization, and fetal development. Int J Mol Sci 10(5):2122–2135

Jiang W, Kim BY, Rutka JT, Chan WC (2008) Nanoparticle-mediated cellular response is size-dependent. Nat Nanotechnol 3(3):145–150

Juan H, XuYing W, Fei W, GuiFeng X, Zhen L, TianBao Z (2009) Effects of titanium dioxide nanoparticles on development and maturation of rat preantral follicle in vitro. Acad J Second Milit Med Univ 30(8):869–873

Kim HR, Park YJ, Shin DY, Oh SM, Chung KH (2013) Appropriate in vitro methods for genotoxicity testing of silver nanoparticles. Environ health toxicol 28:e2013003

Kosmehl T, Krebs F, Manz W, Erdinger L, Braunbeck T, Hollert H (2004) Comparative genotoxicity testing of rhine river sediment extracts using the comet assay with permanent fish cell lines (rtg-2 and rtl-w1) and the ames test. J Soil Sediment 4(2):84–94

Lankveld DPK, Oomen AG, Krystek P, Neigh A, Troost–de Jong AH, Noorlander CW, De Jong WH (2010) The kinetics of the tissue distribution of silver nanoparticles of different sizes. Biomaterials 31(32):8350–8361

Lipka J, Semmler-Behnke M, Sperling RA, Wenk A, Takenaka S, Schleh C, Kreyling WG (2010) Biodistribution of PEG-modified gold nanoparticles following intratracheal instillation and intravenous injection. Biomaterials 31(25):6574–6581

Liu Z, Tabakman S, Welsher K, Dai H (2009) Carbon nanotubes in biology and medicine: in vitro and in vivo detection, imaging and drug delivery. Nano Res 2(2):85–120

Menke AL, Spitsbergen JM, Wolterbeek AP, Woutersen RA (2011) Normal anatomy and histology of the adult zebrafish. Toxicol Pathol 39(5):759–775

Moor C, Lymberopoulou T, Dietrich VJ (2001) Determination of heavy metals in soils, sediments and geological materials by ICP-AES and ICP-MS. Mikrochim Acta 136(3–4):123–128

Nune SK, Gunda P, Thallapally PK, Lin YY, Laird Forrest M, Berkland CJ (2009) Nanoparticles for biomedical imaging. Expert Opin Drug Deliv 6(11):1175–1194

Pan Y, Neuss S, Leifert A, Fischler M, Wen F, Simon U, Jahnen-Dechent W (2007) Size-dependent cytotoxicity of gold nanoparticles. Small 3(11):1941–1949

Pan Y, Leifert A, Ruau D, Neuss S, Bornemann J, Schmid G, Jahnen-Dechent W (2009) Gold nanoparticles of diameter 1.4 nm trigger necrosis by oxidative stress and mitochondrial damage. Small 5(18):2067–2076

Ramsden CS, Henry TB, Handy RD (2013) Sub-lethal effects of titanium dioxide nanoparticles on the physiology and reproduction of zebrafish. Aquat Toxicol 126:404–413

Rathore M, Ray I, Mohanty NC, Maheshwari U, Dayal N, Suman R, Joshi DS (2014) Comparative in vivo assessment of sub-acute toxicity of gold and silver nanoparticles. J Nanopart Res 16:23–38

Schnurstein A, Braunbeck T (2001) Tail moment versus tail length—application of an in vitro version of the comet assay in biomonitoring for genotoxicity in native surface waters using primary hepatocytes and gill cells from zebrafish (*Danio rerio*). Ecotoxicol Environ Saf 49(2):187–196

Singh NP, McCoy MT, Tice RR, Schneider EL (1988) A simple technique for quantitation of low levels of DNA damage in individual cells. Exp Cell Res 175(1):184–191

Singh N, Manshian B, Jenkins GJ, Griffiths SM, Williams PM, Maffeis TG, Doak SH (2009) NanoGenotoxicology: the DNA damaging potential of engineered nanomaterials. Biomaterials 30(23):3891–3914

Stelzer R, Hutz RJ (2009) Gold nanoparticles enter rat ovarian granulosa cells and subcellular organelles, and alter in vitro estrogen accumulation. J Reprod Dev 55(6):685–690

Strober, W. (2001). Trypan blue exclusion test of cell viability. Curr protoc immunol, A3–B

Tiedemann D, Taylor U, Rehbock C, Jakobi J, Klein S, Kues WA, Rath D (2014) Reprotoxicity of gold, silver, and gold–silver alloy nanoparticles on mammalian gametes. Analyst 139(5):931–942

Tsoli M, Kuhn H, Brandau W, Esche H, Schmid G (2005) Cellular uptake and toxicity of Au55 clusters. Small 1(8–9):841–844

Turkevich J, Stevenson PC, Hillier J (1951) A study of the nucleation and growth processes in the synthesis of colloidal gold. Discuss Faraday Soc 11:55–75

Wang C, Yu C (2013) Detection of chemical pollutants in water using gold nanoparticles as sensors: a review. Rev Anal Chem 32(1):1–14

Wang J, Zhu X, Zhang X, Zhao Z, Liu H, George R, Chen Y (2011) Disruption of zebrafish (*Danio rerio*) reproduction upon chronic exposure to TiO_2 nanoparticles. Chemosphere 83(4):461–467

Westerfield M, Institute of Neuroscience (1994) The zebrafish book: a guide for the laboratory use of zebrafish Danio (*Brachydanio rerio*). University of Oregon Press, Corvallis

Zhang XD, Guo ML, Wu HY, Sun YM, Ding YQ, Feng X, Zhang LA (2009) Irradiation stability and cytotoxicity of gold nanoparticles for radiotherapy. Int J Nanomed 4:165–173

Zhu RR, Wang SL, Chao J, Shi DL, Zhang R, Sun XY, Yao SD (2009) Bio-effects of nano-TiO_2 on DNA and cellular ultrastructure with different polymorph and size. Mater Sci Eng C 29(3):691–696